Journal of Applied Pharmaceutical Research
Volume 12 Issue 6, Year of Publication 2024, Page 122 – 136
DOI: https://doi.org/10.69857/joapr.v12i6.661

Check for updates

Research Article

JOURNAL OF APPLIED PHARMACEUTICAL RESEARCH | ***JOAPR***
www.japtronline.com ***ISSN: 2348 – 0335***

FABRICATION AND EVALUATION OF CARBOCISTEINE-LOADED SOLID LIPID NANOPARTICLES TO TREAT PULMONARY INFECTIONS

Bhushan R. Rane, Ashish S. Jain*, Nikita P. Mane, Vaibhav Patil,
Mukesh S. Patil, Kedar R. Bavaskar

Article Information
Received: 19th August 2024
Revised: 11th November 2024
Accepted: 13th December 2024
Published: 31st December 2024

Keywords
Carbocisteine, Solid Lipid Nanoparticle, Particle Size, Stability, Zeta Potential

ABSTRACT
Background: Solid lipids Nanoparticles (SLN) comprise physiological and biocompatible lipids. SLN is an alternative carrier system to polymeric nanoparticles or liposomes. It has been claimed that SLN offers combined advantages and avoids the disadvantages of other colloidal carrier systems. **Aim:** The research aims to fabricate and evaluate the carbocisteine solid lipid nanoparticles loaded in situ gel. **Methodology:** SLN was prepared by using glycerol monostearate as a solid lipid and by high-pressure homogenization (Panda plus 2000) method using poloxamer 188 as a stabilizer to improve its bioavailability and reduce particle size. The quality-by-design concept was used to develop the SLN by optimizing process variables. **Result and discussion:** The drug and excipient compatibility study was checked using FTIR, and no interaction between both was found. Optimized SLN of carbocisteine were evaluated for zeta potential, particle size, and % drug release, found results as -19.67 mv, 50 to 200 nm, and up to 70.84%, respectively. Optimized gel batches were also evaluated for the stability study. **Conclusion:** All the batches were evaluated for various parameters. The F6 batch was optimized based on particle size, stability, Zeta potential, and release pattern. SLN could provide a better advantage of good penetration and targeting to treat pulmonary disease.

INTRODUCTION

Novel drug delivery systems are developing exponentially due to the deep understanding obtained in various biotechnology, nanotechnology, and biomedical engineering domains. Many more modern formulation techniques use nanotechnology, which creates nanoscale structures that hold the API. The National Nanotechnology Initiative (NNI) defines nanotechnology as the study and application of structures generally between 1 and 100 nm in size [1-5]. Solid lipid nanoparticles introduced in 1991 offer an improved substitute for conventional colloidal carriers like polymeric micro and nanoparticles, liposomes, and emulsions [1]. Solid lipid nanoparticles are colloidal carrier systems comprising an aqueous coating over a solid core of a high melting point lipid. Solid lipid replaces liquid lipid in solid lipid nanoparticles compared to other colloidal carriers [7-10]. Since lipid pellets are administered via the oral route (Mucosolvan®) to deliver the drug, solid lipids are usually used as a matrix material. All lipids are triglycerides, partial glycerides, fatty acids, hard fats, and

*Department of Pharmaceutics, Shri D. D. Vispute College of Pharmacy & Research Center, Panvel, Dist. Raigad, India 410206

***For Correspondence:** **drashishjain80@gmail.com**

waxes. One clear advantage is that the lipid matrix of solid lipid nanoparticles comprises physiological lipids, which reduces the possibility of both acute and long-term toxicity [11]. It has been demonstrated that using solid lipids rather than liquid lipids improves the stability of integrated chemically-sensitive lipophilic components and increases control over the release kinetics of encapsulated substances. Numerous physicochemical traits connected to the lipid phase's physical state are responsible for these potentially advantageous impacts [12-13]. First, compared to a liquid matrix, a solid matrix has less reactive agent mobility, which could slow the rate of chemical degradation processes [14-16]. Second, it is possible to regulate the microphase separations between the carrier lipid and active components within individual liquid particles. This prevents the buildup of active compounds at the lipid particle surface, which is a common site for chemical degradation reactions. Thirdly, it has been demonstrated that incorporating poorly absorbed bioactive chemicals into solid lipid nanoparticles increases their absorption [15-20].

The primary feature of chronic obstructive pulmonary disease (COPD), which is a significant cause of death and morbidity in both industrialized and developing nations, is a gradual airflow restriction that is not entirely reversible [21, 22]. Globally, there are significant differences in COPD prevalence [23]. COPD is a widespread condition in the elderly population, with a higher incidence rate among those over. The Burden of Obstructive Lung Disease (BOLD) study indicated that 10.1% of people had COPD overall, defined as GOLD stage II or higher. The prevalence was 11.8 percent for men and 8.5 percent for women. The most common sign of COPD is a progressive deterioration in lung function, often accompanied by respiratory symptoms such as coughing, sputum production, and dyspnoea [23-28].

Carbocisteine is the most often administered mucoactive drug for long-term COPD patients. Mucolytic carbocisteine helps patients with bronchiectasis and chronic obstructive pulmonary disease (COPD) by reducing the viscosity of their sputum and making it easier for them to cough up secretions. Some of the issues with carbocisteine, such as its low oral bioavailability (around 10%), may make it difficult for patients to follow their treatment plans, which could result in therapeutic failure [26-30]. Hence, to overcome such challenges of carbocisteine delivery, SLNs are preferred because of their properties such as [31]

1. Possibility of controlled drug release and drug targeting.
2. Increased drug stability
3. High drug payload
4. Incorporation of lipophilic and hydrophilic drugs
5. No biotoxicity of the carrier
6. Avoidance of organic solvents
7. Increased Bioavailability of entrapped bioactive compounds

This study aims to produce and optimize an intranasal formulation for nasal distribution by integrating carbocisteine solid lipid nanoparticles into the in-situ gel. The research seeks to create nasal gels filled with medication formulations poorly soluble in water for intranasal administration. The study's rationale was to increase the bioavailability and reduce the drug dose to minimize the side effects by targeting a specific site through intranasal drug delivery.

MATERIALS AND METHODS

Carbocisteine was received as a sample for work by MicroLabs Mumbai, India. Poloxamer 188, tween 80, glyceryl monostearate, tween 20, gellan gum, xanthan gum, propylene glycol, and triethanolamine were purchased from Research-Lab Fine Chem Industries, Mumbai.

FTIR Analysis

The FTIR instrument (Shimadzu, IR Affinity—IS CE) is used for FTIR investigations. The FTIR spectra and peak table were acquired after the sample was placed in the detecting area [32].

Preparation of SLN loaded with carbocisteine

A high-pressure homogenization process (GEA Niro Soavi Italy, Panda Plus 2000 homogenizer) prepared carbocisteine-loaded solid lipid nanoparticles. A solid lipid nanoparticle was generated at 500–1500 bars following five to ten homogenization cycles. 5 min to 8 min are required per cycle. The formation of solid lipid nanoparticles loaded with carbocisteine involved varying concentrations of surfactant [33]. Compared to Tween 80 and Tween 20, poloxamer 188 can form smaller particles.

Compared to Tween 80 and Tween 20, poloxamer 188 has a higher molecular weight and HLB value. Poloxamer 188 was utilized as a stabilizer, surfactant, and detergent, as shown in **Table 1**. The melting point of various amounts of glyceryl monostearate was raised by 5 to 10 ^{0}C. Multiple studies showed

that combining poloxamer 188 and glyceryl monostearate (GMS) can produce solid lipid nanoparticles (SLNs) with smaller particle sizes. As the lipid core, glyceryl monostearate was employed [34]. Carbocisteine was put into the liquefied fat. Separately, an aqueous phase containing surfactant was dissolved using distilled water. It was done to raise the temperature of the aqueous phase to that of the oil phase. Subsequently, the aqueous and oil phases were combined extensively [35].

The resulting coarse emulsion was homogenized at a constant temperature of 75°C using a high-pressure homogenizer. Consequently, the nanoparticles are formed when the nanoemulsion is finally cooled to room temperature, which causes the lipids to recrystallize, as demonstrated in **Figure 1**.

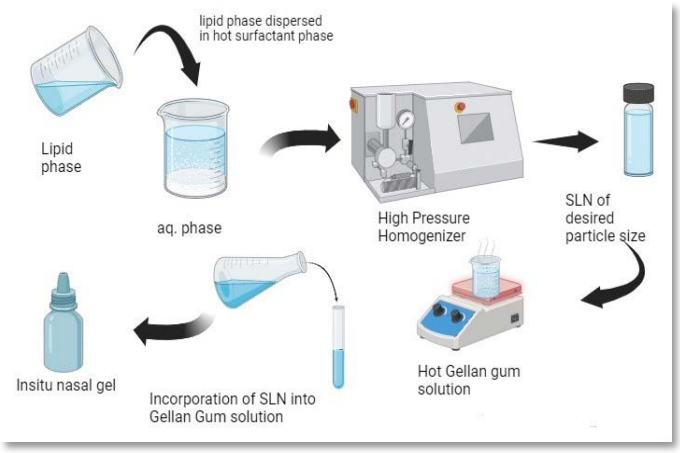

Figure 1: Schematic representation of preparation Carbocisteine solid lipid nanoparticle loaded in-situ nasal gel

Table 1: Formulation table of Carbocisteine Solid lipid Nanoparticles

Batch code	Drug (mg)	GMS (mg)	Tween 80	Poloxamer 188	Tween 20
F1	100	100	1%	-	-
F2	100	150	1.5%	-	-
F3	100	200	2%	-	-
F4	100	100	-	1%	-
F5	100	150	-	1.5%	-
F6	100	200	-	2%	-
F7	100	100	-	-	1%
F8	100	150	-	-	1.5%
F9	100	200	-	-	2%

Optimization of formulation

Selection of formulation variables

Solubility experiments were used to screen various lipids. The drug's solubility in various lipids was assessed. The amount of medication dissolved in a known quantity of each lipid at 5°C above the lipid's melting point was calculated. The chosen lipid was used to form nanoparticles using various surfactants, which were then assessed for entrapment effectiveness, PDI, and particle size. The Malvern Zetasizer Nanoseries Nano-ZS was used to measure the particle size and PDI. The surfactant was used to choose the minimal particle size and PDI with the highest entrapment efficiency. Two levels (+1 and −1) of the concentration of lipid, concentration of surfactant, and Pressure of homogenizer (independent variables) were selected as shown in **Table 2.** DOE software (Version 13.0.5.0) was used to design the experiments. Table 3 displays the design arrangement. The software created 13 formulas in total [35].

Table 2. Independent Variable

Independent Variables	Level	
	+1	-1
A: Conc. of lipid (mg)	100	200
B: Conc. of poloxamer (%)	1	2
C: Pressure of HPH (bar)	500	1000

Statistical analysis

Design Expert® software was utilized in conjunction with the analysis of variance (ANOVA) to analyze the variables statistically. The effects and interactions of the formulation factors on the results were examined [36]. Design Expert® program used sequential p-value, lack of fit p-value, modified R^2, and predicted R^2 to get the best-fitting model. P-values less than 0.05 and F-values higher than 0.05 signify a significant impact from every component. Counter and three-dimensional surface graphs can depict the relationship between causes and consequences. A decreasing effect on the response in a polynomial equation is denoted by a negative sign for the coefficient's magnitude and a rising effect by a positive sign [37].

Selection of optimized formulation

Optimizing the carbocisteine-solid lipid nanoparticles allowed for the best feasible particle size and entrapment efficiency. An overlay plot produced by a graphical method and a numerical approach based on a desired function that ranges from 0 to 1

were used for optimization. The predicted values of the variables with the highest desire function were used to generate the best formulation. The actual outcomes were contrasted with the expectations [38].

Characterization of SLN

Particle Size

The Malvern Nano-ZS laser scattering technology subjected solid lipid nanoparticles to particle size measurement. The nanoparticles were dispersed in an aqueous solution to minimize particle contact and put in an agitated sample dispersion unit. The particle size analysis spectrum is the mean of three scans conducted at 25°C. The system gives the mean particle size and the polydispersity index [39].

Zeta Potential

The zeta potential was determined using Malvern Nano-ZS. At 25°C, the best signal intensity was obtained by diluting with water six to eight times before analysis. We noted and further evaluated the average value [39].

Transmission Electron Microscopy

Transmission electron microscopy (TEM) was used to measure the size of the particles. Solid lipid nanoparticles were then optimized by their shape, and the pressure in the bar was adjusted. After placing them on a sheet covered in carbon, a sufficient sample was left over to allow the solid lipid nanoparticles to adhere to the carbon substrate. After that, the grid was dyed with phosphotungstate for 20 seconds. An infrared lamp was used to dry the produced sample before being examined using a TEM (Model: TEM-FEI, Tecnai G2 Spirit Biotwin). The Soft Imaging Viewer software captured the photos at different magnifications [40, 41].

Entrapment Efficiency

The carbocisteine-loaded nanoparticles were separated from the aqueous suspension for 20 minutes at 10,000 rpm and 4 °C in a cooling centrifuge (Remi C24 Plus). Following the supernatant collection, the drug concentration was determined at the appropriate dilutions using the HPLC technique. [42].

Table 3. Variables and responses of Box Behnken Design-selected compositions of variables

Run	Factor 1	Factor 2	Factor 3	Response 1	Response 2
	A: Conc. of lipid (mg)	B: Conc. of poloxamer (%)	C: Pressure of HPH (bar)	EE (%)	Particle size (nm)
1	200	1	750	60.31	130.76
2	150	1	1000	56.91	110.2
3	100	1	750	42.8	161.55
4	150	1.5	750	47.84	139.62
5	200	1.5	750	64.58	135.22
6	200	2	1000	70.22	94.23
7	100	2	750	50.23	167.95
8	100	1.5	1000	44.33	160.43
9	150	2	500	62.18	152.46
10	100	1.5	500	45.61	158.9
11	150	2	1000	66.69	102.33
12	150	1	500	44.65	155.53
13	200	1.5	500	63.61	142.56

Preparation SLN loaded in situ nasal gel.

Gellan gum was dissolved in distilled water at concentrations of 0.25%, 0.5%, and 1% w/v. It was then heated to 90 °C with moderate stirring (Remi, Mumbai, India) and cooled. Concurrently, distilled water was mixed with xanthan gum 0.15% [43]. After centrifuging the solid lipid nanoparticles, the

resulting pellet was gradually stirred into the xanthan gum solution. This resultant solution was assessed after being combined with gellan gum solution [44].

Characterization of solid lipid nanoparticles loaded in-situ nasal gel.

pH

The pH of the gel formulation was ascertained by preparing a 1% aqueous solution and storing it for an hour. The pH was measured using a digital pH meter (Hanna Italy, Probe type). The calculation was done three times to ensure accuracy, yielding an average value plus standard deviation [45, 46].

Clarity

The clarity of the generated in-situ gels was evaluated visually against a black and white backdrop, and the results were scored as follows: turbid, +; clear, ++; and very clear (glassy), +++ [47].

Spreadability

The area that the sol-gel formulation covers in a minute at a time (cm2/min) is known as spreadability. The spreadability of the formulations was evaluated using Whatmann's filter paper [48]. A 1 mL graduated pipette tip with a rubber bulb was attached vertically to the stand so the tip was 2 cm above the filter paper's rounded horizontal surface. A drop of 0.1 mL of the sol formulation was placed in the center of the filter paper. At predetermined intervals of 20 seconds, the surface area covered by the formulation was measured. [49, 50].

Gelling time

By introducing in situ gel (1 mL) (n = 3) to a predetermined amount of simulated nasal fluid, the gelling time was ascertained, and the amount of time required for the gel to form was noted [51, 52].

Viscosity

The viscosity of in situ gel was measured using a Brookfield viscometer (viscometer Model DV2T) both before and after gelation. Viscosity was measured at neutral pH before and after gelling (at SNF pH 5.5–6.5). [53-54].

Drug content

The in-situ gel was spread out in 20 mL of water, and 1 gram gel was dissolved entirely by shaking the water continuously. HPLC was used to determine the drug concentration, and water was added to bring the volume down to 50 mL [54].

In vitro mucoadhesion studies

The texture analyzer (Brookfield Engineering Laboratories, Inc., Massachusetts, USA) and a mucoadhesive holder were used to measure the in-situ gel's mucoadhesive strength. Measuring approximately 10 mm by 10 mm, the sheep nasal mucosa was immersed in 20 mL of the nasal fluid substitute and left to acclimate at 32±2°C for 10 minutes. Twenty milligrams of in situ gel were applied to the mucoadhesive holder. At a speed of 0.5 mm/s, the probe was lowered until it made contact with the membrane. After maintaining a contact force of 1N for 30 seconds, the probe was then withdrawn at a speed of 0.5 mm/s to a distance of 20 mm [55-57].

Using Texture Pro CTV1.3 Build 14 software, it is possible to immediately record the maximum force necessary to separate the probe from the tissue (also known as the maximum detachment force in grams, or Fmax [58-60]. The following formula is used to determine mucoadhesive strength:

Mucoadhesive strength dyne / cm^2 = m.g/A Eq 1

Where A is the exposed tissue area (cm2), g is the acceleration caused by gravity (980 cm/s2), and m is the weight needed for detachment (g).

Critical ionic concentration for phase transition

The critical ionic concentration was established through the mixing of one milliliter of formulation with varying amounts of simulated nasal fluid containing Sodium chloride-7.45 mg/mL, Potassium chloride-1.29 mg/mL, and Calcium chloride-0.32 mg/mL at a pH of 6.5 in vials. After 20 seconds, the vials were inverted and monitored for gel formation. The minimum volume of nasal fluid necessary for the gel to adhere to the vial bottom without sliding was noted. This volume represented the critical ionic concentration, determined by assessing the concentrations of different ions within the required nasal fluid volume [60,61].

Gel strength

A 100 cm3 graduated cylinder containing 35 g of the formulation was used for measurement, A 20 g piston was carefully placed into the gelled solution and given a free region to penetrate 3 cm^3 of gel. The amount of time it took for the weight to sink 3 cm3 was measured in seconds, and this number is directly related to the gel strength [61].

Nasal ciliotoxicity studies

Studies on nasal ciliotoxicity were conducted using recently isolated sheep nasal membranes taken from the slaughterhouse. Following saline solution cleaning, the membrane section was treated with, optimized in situ gel, isopropyl alcohol (as a positive control), and phosphate buffer pH 6.4 (as a negative control). Following an 8-hour duration, distilled water was used to wash each sample, and hematoxylin and eosin were used for staining. Each segment was inspected using an optical microscope (Labline) to look for any signs of membrane damage [61].

Stability Study

According to ICH recommendations, the optimized gel was stabilized at 40ºC and 75% RH for three months. For 1, 2, and 3 months, the gel was kept in a dry, clean, airtight, moisture-proof glass vial sealed with rubber covers and kept out of direct sunlight. The stability of the optimized solid lipid nanoparticle in-situ gel was assessed monthly to look for any changes based on measurements of the drug content percentage, PH, viscosity, and in vitro release [61].

In vitro Release

Franz diffusion cells were utilized for in vitro testing of produced formulations. The diffusion membrane kept the recipient and donor compartments apart. In the donor compartment, prepared formulations are stored, while in the recipient compartment, simulated nasal fluid (SNF) is maintained at 37 ± 0.5 °C. One mL sample was removed from the receptor compartment and replaced with fresh SNF at predefined intervals to keep the sink condition. After removing the samples, they were filtered, and the amount of medication that had entered was measured using a UV-visible spectrophotometer set to λ max 220 nm [62, 63]. A study compared the drug solution, optimized in situ gel, and solid lipid nanoparticles [63].

RESULTS AND DISCUSSION

FTIR Analysis

FTIR was used in the preformulation investigation to assess the optimized formulation's and carbocisteine compatibility. The C-H stretching was detected at 1161.15 cm−1 in the Carbocisteine FTIR spectra. The measured C=O stretching was 1627.92 cm−1. At 1195.87, the O-H stretching was discovered. The C-S stretching-attributed peaks were detected at 1033.85 cm−1 and 958.62 cm−1. The observed peaks confirm the drug's purity, aligning with the typical reported peaks.

The peak at 1159.22 cm−1 in the Optimized formulation's FTIR spectrum is similar to the C–H stretching. The length of the C=O is 1631.78 cm−1. O-H stretching is responsible for the peaks seen at 1197.79, whereas C-S stretching is at 1031.92 and 889.18 cm−1. The medication in the optimal formulation is validated similarly to all of the peaks shown above. Consequently, FTIR analysis shows that the medication is compatible with the formulation and does not interact with any excipients, as shown in **Figure 3**.

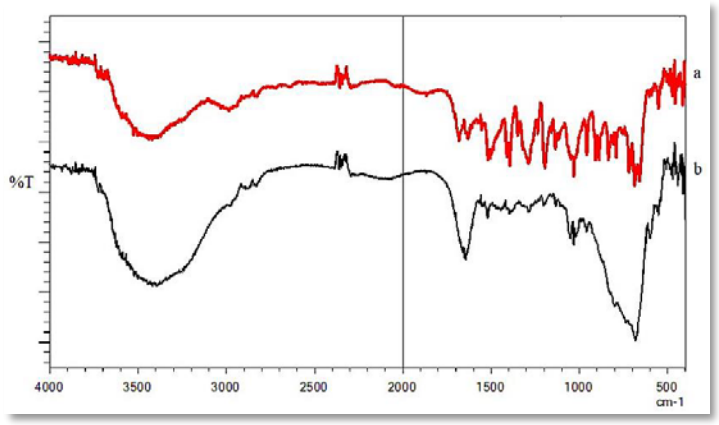

Figure 3: FTIR analysis of **a**. Drug (Carbocisteine) **b**. Optimized formulation.

Experimental design optimization and response surface approach statistical analysis

Statistical analysis

The experiment design results showed that the amount of lipid, surfactant, and homogenizer pressure significantly impacted this system, leading to high drug EE and small particle sizes during the solid lipid nanoparticle manufacturing process. The model for response analysis was chosen based on the evaluation of multiple statistical parameters, such as Sequentia p-values, projected R^2, and adjusted R^2. The selected model should have a lower predicted R^2 value, adjusted R^2 value, and sequential p-values. Three independent variables were chosen for analysis, and a linear model was used. The polynomial equations (Linear) of each response generated from the software are given below;

Entrapment efficiency (Y1) = 55.3815 + 9.46875 * A + 5.31905 * B + 2.09762 * C

Particle size (Y2) = 255.247 + -0.36515 * A + -5.91429 * B + -0.0696514 * C

P-values less than 0.0500 indicate model terms are significant.

Table 4. Statistics model summary of responses of Carbocisteine solid lipid nanoparticles

Response (Y1)	**Sequential p-value**	**Adjusted R^2**	**Predicted R^2**
Linear	**0.0002**	**0.8297**	**0.7621**
2FI	0.7276	0.7913	0.6575
Quadratic	0.6450	0.7433	-1.4011
Response (Y2)			
Linear	**0.0038**	**0.6800**	**0.4812**
2FI	0.3929	0.6981	0.2272
Quadratic	0.3563	0.7668	-1.2375

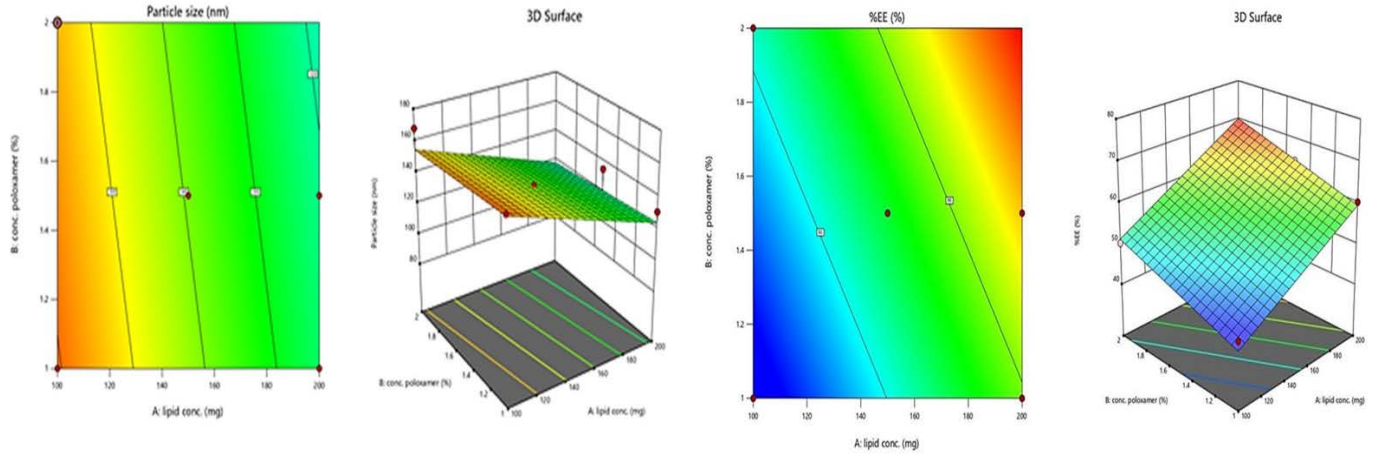

Figure 4: Effect of independent variables on particle size and EE

Effect of independent variables on particle size

It was discovered that the particle size of solid lipid nanoparticles ranged from 94.23 nm to 167.95 nm. Figure 4's polynomial equation 3D plot and contour plot demonstrated how a variable affected particle size. The size of the solid lipid nanoparticles rose from 2 to 6% lipid content. Particle aggregation caused the size to increase. The size of the solid lipid nanoparticles reduced as the concentration rose from 1 to 4%. The size drop may result from decreased interfacial tension between two phases, slowing down particle agglomeration.

Effect of independent variables on EE

Each experimental run of solid lipid nanoparticles was subjected to centrifugation to evaluate its EE; the results are presented in Table 3. The range of EE was found to be 42.8% to 70.22%. The effects of variables on the EE were shown using polynomial equations, 3D plots, and contour plots, as shown in Figure 4. Increasing the surfactant content from 1% to 3% causes a rise in EE. The rise in EE results from an increase in the amount of space available to entrap the carbocisteine into the lipid matrix.

Characterization of solid lipid nanoparticles loaded with carbocisteine.

Particle Size

The optimal particle size range for efficient pulmonary delivery is between 1 and 5 micrometers. This size of particle can successfully enter the lungs' deep chambers without becoming stuck in the upper respiratory system. The smaller particles have a higher surface area-to-volume ratio, which can improve drug absorption and solubility. When the medication enters the pulmonary tissue, this may result in increased bioavailability.

The particle size of all prepared formulations was measured. The optimized batch of SLN created had a particle size of 97.23 nm. While raising the concentration of Poloxamer 188 has an impact, increasing the lipid content (GMS) does not affect particle size. **Figure 5** shows the particle size of dispersion.

Polydispersibility index

The Polydispersibility index of prepared SLN was 0.212, indicating that the prepared solid lipid nanoparticles are homogeneous.

Zeta Potential

Strong electrostatic repulsion between particles is indicated by a high absolute zeta potential, which can be either positive or negative. This helps to avoid sedimentation and aggregation. For medication compositions to remain consistent, this stability is essential. The way nanoparticles interact with the nasal mucosa is influenced by zeta potential. Formulations with the ideal zeta potential can improve drug absorption by improving adherence to the mucosal surface. For example, negatively charged mucosal surfaces may interact with positively charged nanoparticles more efficiently, lengthening retention time. **Figure 6** shows the zeta potential of the batch ranging from -19 mV, meaning that the formulation is stable based on the zeta value and its standard deviation.

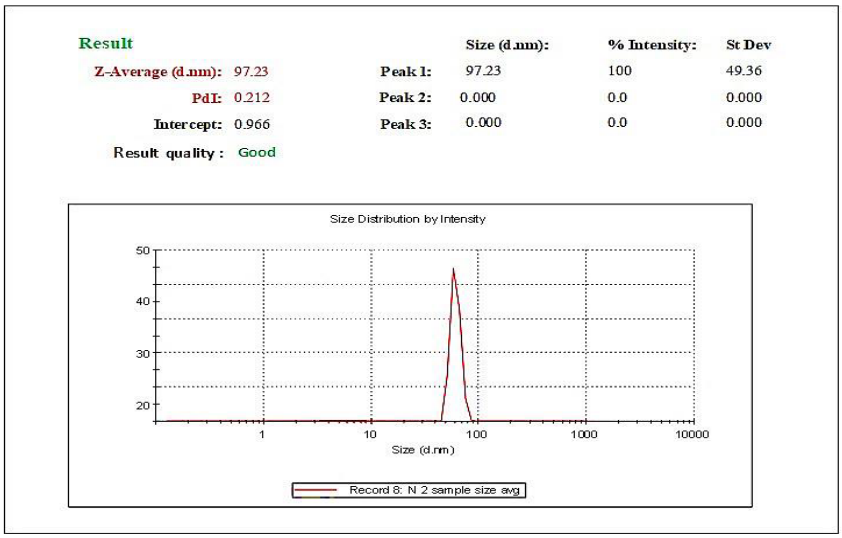

Figure 5: Zeta Size image of optimized Formulation

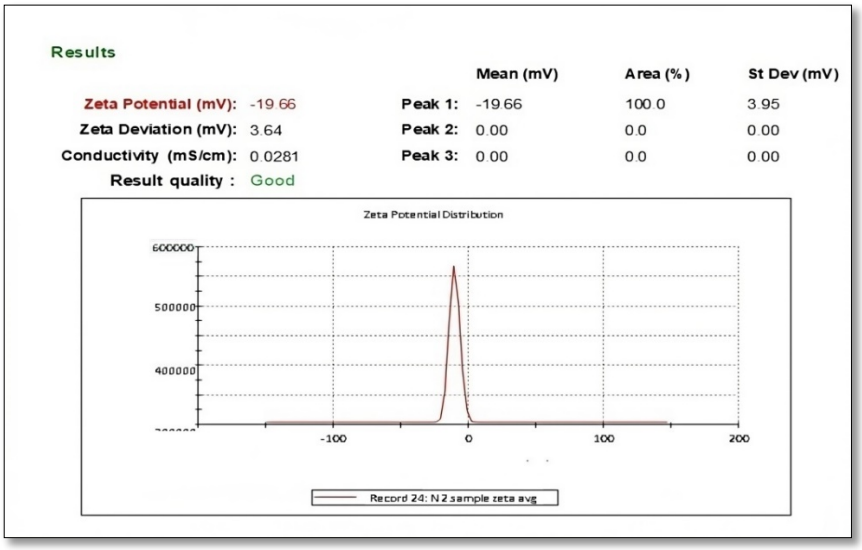

Figure 6: Zeta Potential image of Optimized Formulation

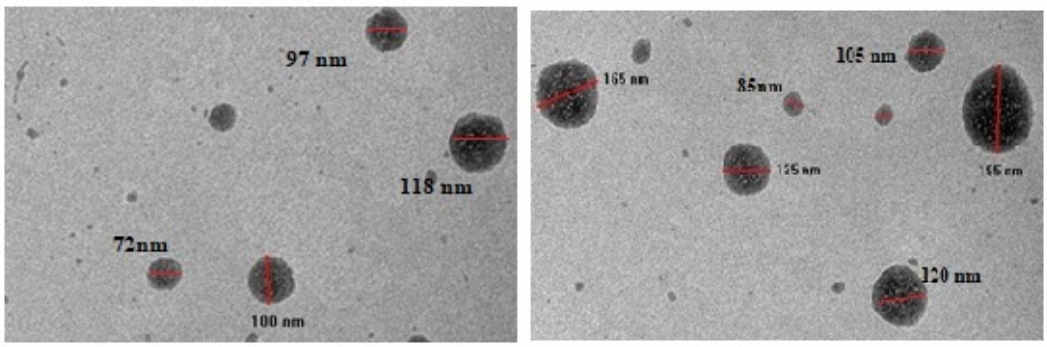

Figure 7: TEM image of optimized solid lipid nanoparticle formulation

Transmission Electron Microscopy

The shape of SLN influences absorption and bioavailability by affecting the residence period and the interaction with the nasal mucosa. Spherical particles typically have lower clearance rates and more predictable diffusion through mucus, but smaller particles' greater surface area may improve drug absorption and release rates. Because they can better permeate the mucosal membrane and increase bioavailability, particles typically in the 50-200 nm range are preferred for intranasal delivery. The size of solid lipid nanoparticles was measured using Transmission Electron Microscopy (TEM) (Jeol/JEM 2100), and the photos below depict its structure. We can infer from Figure 7 that the improved formulation includes nanoparticles smaller than 200 nm.

Entrapment Efficiency

An increase in surfactant concentration was shown to result in an increase in entrapment efficiency during the trials. **Figure 8** presents the entrapment efficiency values for each formulation that was prepared. In summary, Optimized formulation exhibits the highest entrapment rate of 68.28%, leading us to this conclusion. Studies have shown that poloxamer 188 has high conc. Batch produces the best outcomes. Many formulations in the literature report EE values ranging from 30% to 60%. Highlighting that the formulation achieves up to 68.28% EE demonstrates a significant improvement. Therefore, F6 is being considered for the in-situ nasal gel formulation of Solid lipid nanoparticle loaded.

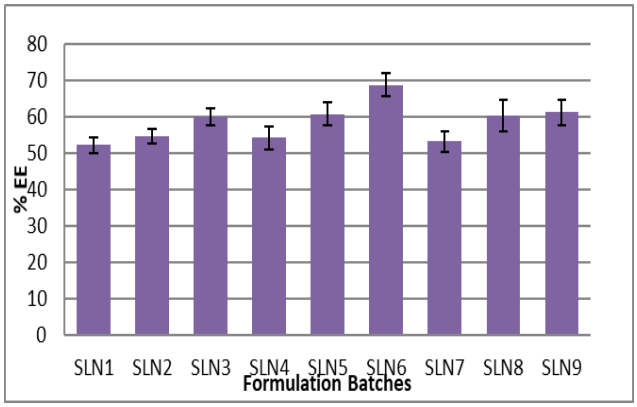

Figure 8: Entrapment efficiency of Solid lipid nanoparticle batches

Characterization of SLN Loaded In-situ Nasal Gel

pH

The drug's ability to penetrate the nasal mucosa can be influenced by the formulation's pH and its pKa. The gel's pH might impact the interactions between polymers necessary for gel formation. As seen in **Table 5**, the pH range of the created formulations is 5.9 to 5.5, which is within the nasal pH range. This suggests that all in-situ gels can accommodate nasal pH to reduce irritation during administration.

Spreadability

The in-situ gel must have the right spreadability to be applied smoothly and adhere to the nasal mucosa without leaking after application. Compared to SLNG2 and SLNG3, SLNG1 exhibits better spreadability from prepared in-situ gel, as per Table 5.

Clarity

Visual inspection assessed the clarity of the created in-situ gels, and SLNG1 had significantly more clarity than SLNG2 and SLNG3, as per **Table 5**.

Drug Content

Every dosage form is thought to need to have uniform medication content. As shown in **Table 5**, the drug content of each batch varied from 97.27 ± 1.5% to 98.29 ± 1.2%. It was discovered that SLNG1 had higher drug content.

In Vitro Gelation Study

Gelation tests were conducted using an adequately prepared synthetic nasal fluid. For each generated formulation displayed in Table 4, gelation takes place in 50 seconds. Compared to SLNG2 and SLNG3, SLNG1 is quicker to finish. It states, thus, that in-situ generated gel retains its integrity without dissolving or degrading to localize the medication to the absorption site for an extended period or to resist mucociliary clearance. The research above makes it evident that SLNG1 was shown to be a superior formulation. Thus, SLNG1 is considering the viscosity and in vitro release tests.

Mucoadhesive strength

Mucoadhesive polymers prolong the duration of the drug's presence in the nasal cavity by facilitating its interaction with the nasal mucosa, which can improve the drug's bioavailability and therapeutic activity. This is because the drug can bypass the first-pass metabolism and the gastrointestinal tract. For formulations, mucoadhesive strength testing was done; the results are shown in **Table 5**. Stronger mucoadhesive forces can potentially hinder drug absorption by preventing gelled solutions from draining into the nasopharynx and out of the nasal cavity.

Viscosity

The developed formulations demonstrate that viscosity rises as gelling agent concentration does. Because of ionic interaction, viscosity needs to be at its peak and quickly transition from a sol-gel state to introduce the formulation into the nasal cavity. Therefore, unlike the others, the SLNG1 satiated the viscosity requirements. All the results are shown in **Table 5**.

Critical ionic concentration for phase transition

The simulated nasal fluid's constituents interact ionically with the gellan gum to form a gel. Therefore, determining the critical ionic concentration needed for gel formation is crucial. As shown in **Table 5**. the critical ionic concentration for each batch ranged from 0.30 ± 0.05 to 0.40 ± 0.02%. At 0.30 ± 0.03 mL, the optimized batch (SLNG1) had a critical ionic concentration.

Gel strength

The in-situ gel formulae SLNG1, SLNG2, and SLNG3 had gel strength values that roughly dropped between 10 and 34 seconds, as shown in **Table 5**. This range is suitable for intranasal instillation because values higher than 50 seconds are too stiff and could harm or cause discomfort to the mucosal surfaces. Conversely, values less than 25 seconds would not be able to retain their integrity and could erode quickly. The rise in in-situ gel strength may be due to the creation of hydrogen bonds between Poloxamer and the bioadhesive polymers employed in the formulation.

Table 5. Different parameters studies of prepared in situ gel

Parameters Evaluated		**Formulation code**		
		SLNG1	SLNG2	SLNG3
Clarity		+++	++	++
Drug Content (%)		98.29 ± 1.2%	97.13 ± 1.3%	97.27 ± 1.5%
pH		5.5	5.7	5.8
Gelation Time (s)		46 ± 1.5	47 ± 1.4	50 ± 1.3
Spreadability (cm2)		1.607 ± 0.5	1.450 ± 0.4	1.320 ± 0.3
Mucoadhesive strength (Dyne/cm^2)		4430	4018	4214
Viscosity (cp)	Before Gelation	72.0 ± 1.2	64.0 ± 1.4	53.0 ± 1.3
	After Gelation	274.0 ± 4.8	178.0 ± 5.9	133.0 ± 5.3
Critical ionic concentration (%)		0.30 ± 0.05	0.39 ± 0.06	0.40 ± 0.02
Gel Strength (sec)		34.6 ±1.53	27.3 ±0.57	10.3 ±1.15

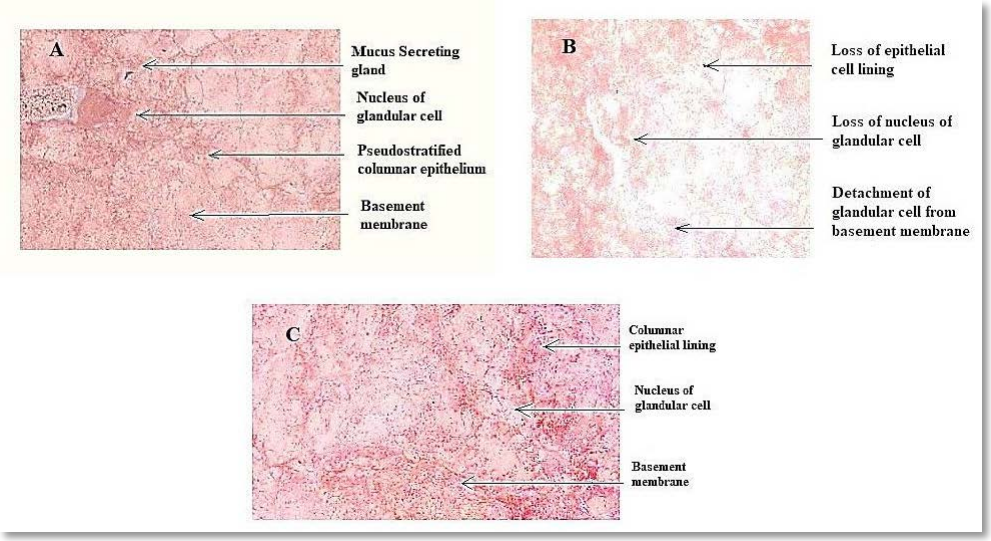

Figure 9 A. The nasal tissue was treated with PBS at pH 6.4 B. The nasal tissue treated with IPA C. The nasal tissue treated with SLN-based in situ gel

Nasal ciliotoxicity study

These investigations evaluate the potential toxicity of the formulation's components to the nasal mucosa. As shown in Figure 9A, PBS pH 6.4-treated nasal tissue displayed an intact basement membrane with glandular cells and a neuroepithelial layer. The positive control, IPA, caused substantial damage to the nasal tissue, as seen in **Figure 9B**.

This damage included the loss of the epithelial layer, the detachment of glandular cells from the basement membrane, and the loss of the glandular cells' nucleus. The nasal tissue exposed to the carbocisteine SLN-based in-situ gel shown in Figure 9C did not show damage to the basement membrane, epithelial layer, or glandular cell nucleus, further confirming the safety of making in-situ gel. It follows that using SLN-based in situ gel via the nasal route is safe.

Stability study

A stability study was performed as per ICH guidelines. The optimized formulation was subjected to a three-month stability testing at a temp of 40ºC & 75% RH**.** The results are shown in **Table 6**. The pH of the gel formulations chosen for the accelerated stability analysis was consistent with the initial observations made at the start of the investigation. Throughout and after the accelerated research period, these formulations showed acceptable in vitro release and viscosity. The formulation was stable after storage at temp 40ºC & 75% RH.

Table 6. Stability studies of optimized formulation

Time (Months)	**(Temp. 40ºC & 75% RH)**			
	PH	**Viscosity (cp)**		**In vitro release (%)**
		Before Gelation	**After Gelation**	
Initial	5.5± 0.23	72.0 ± 1.2	274.0 ± 4.8	85.97 ± 2.34%
1	5.5± 0.26	72.0 ± 1.5	275.0 ± 5.6	83.72 ± 3.04 %
2	5.5± 0.32	73.0± 1.5	275.0 ± 4.9	82.43 ± 2.17%
3	5.5± 0.37	74.0± 1.3	276.0± 5.8	82.11 ± 2.12%

In Vitro Release

The results indicate that the drug solution released was 50.32 ± 2.05% in 6 hrs, while the solid lipid nanoparticle release was around 70.80 ± 2.55% in 10 hrs. The final formulation demonstrates a maximum release of 85.97 ± 2.34% in 12 hrs. According to this comparison of drug release, producing a nanoform increases drug penetration while decreasing drug particle size.

CONCLUSION

The current research work explored the development of carbocisteine solid lipid nanoparticle loaded in-situ gel for nasal delivery using gellan gum, an anionic natural polymer., optimized by the systematic approach of design of experiments (DoE), and assessed for their effectiveness in pulmonary targeting. The response surface methodology's selected experimental design, such as the Box-Behnken design, is a mathematical model that generates an optimal formulation. Optimized formulation was prepared, and particle size for the optimized batch was less than 100 nm, EE 68.28%, and Drug release at 60 min70.84 ± 2.12% respectively; this approach can be used in the future to improve therapeutic efficacy and bioavailability, demonstrating better results for intranasal distribution. The sol-gel transformation took less than 50 seconds. This implies that the medicine can be delivered directly to the pulmonary system through the nose using carbocisteine-loaded SLN-based in-situ gel. The current study is anticipated to aid researchers in forming an in-situ gelling system for pulmonary distribution, which will increase the effectiveness of therapies for lung-related illnesses and improve the bioavailability of oral medications. Future steps to ensure the effectiveness of these treatments include in vivo Studies. Once in vivo studies demonstrate promising results, the next step would be to initiate clinical trials and mechanistic studies. The potential of SLN-loaded in situ gels for treating pulmonary diseases can be better understood and confirmed by addressing these next steps, opening the door for beneficial clinical applications.

FINANCIAL ASSISTANCE

NIL

CONFLICT OF INTEREST

The authors declare no conflict of interest.

AUTHOR CONTRIBUTION

Bhushan R. Rane, Nikita P. Mane, and Vaibhav Patil conceived and designed the study and wrote the manuscript. They also conducted the research, contributed to data collection, and wrote the manuscript. Bhushan R. Rane, Mukesh S. Patil, Kedar R. Bavaskar, and Ashish S. Jain have reviewed and edited the manuscript for clarity, grammar, and consistency.

REFERENCES

[1] Paliwal R, Paliwal SR, Kenwat R, Kurmi BD, Sahu MK. Solid lipid nanoparticles: a review on recent perspectives and patents. *Expert Opin Ther Pat*, **30(3)**, 179-94 (2020) https://doi.org/10.1080/13543776.2020.1720649.

[2] Costa CP, Barreiro S, Moreira JN, Silva R, Almeida H, Sousa Lobo JM, Silva AC. In vitro studies on nasal formulations of nanostructured lipid carriers (NLC) and solid lipid nanoparticles (SLN). *Pharmaceuticals*, **14(8)**,711 (2021) https://doi.org/10.3390/ph14080711.

[3] Bhagwat GS, Athawale RB, Gude RP, Md S, Alhakamy NA, Fahmy UA, Kesharwani P. Formulation and development of transferrin targeted solid lipid nanoparticles for breast cancer therapy. *Front Pharmacol*, **27(11)**, 614290 (2020) https://doi.org/10.3389/fphar.2020.614290.

[4] Pandian SR, Pavadai P, Vellaisamy S, Ravishankar V, Palanisamy P, Sundar LM, Chandramohan V, Sankaranarayanan M, Panneerselvam T, Kunjiappan S. Formulation and evaluation of rutin-loaded solid lipid nanoparticles for the treatment of brain tumor. *Naunyn Schmiedebergs Arch Pharmacol*, **394**,735-49 (2021) https://doi.org/10.1007/s00210-020-02015-9.

[5] Sakellari GI, Zafeiri I, Batchelor H, Spyropoulos F. Formulation design, production and characterisation of solid lipid nanoparticles (SLN) and nanostructured lipid carriers (NLC) for the encapsulation of a model hydrophobic active. *Food Hydrocoll Health*, **1(1)**,100024 (2021) https://doi.org/10.1016/j.fhfh.2021.100024.

[6] Shah P, Chavda K, Vyas B, Patel S. Formulation development of linagliptin solid lipid nanoparticles for oral bioavailability enhancement: role of P-gp inhibition. *Drug Deliv Transl Res*, **11**, 1166-85 (2021) https://doi.org/10.1007/s13346-020-00839-9.

[7] Hassan H, Adam SK, Alias E, Meor Mohd Affandi MM, Shamsuddin AF, Basir R. Central composite design for formulation and optimization of solid lipid nanoparticles to enhance oral bioavailability of acyclovir. *Molecules*. **26(18)**, 5432 (2021) https://doi.org/10.3390/molecules26185432.

[8] Mura P, Maestrelli F, D'Ambrosio M, Luceri C, Cirri M. Evaluation and comparison of solid lipid nanoparticles (SLNs) and nanostructured lipid carriers (NLCs) as vectors to develop hydrochlorothiazide effective and safe pediatric oral liquid formulations. *Pharmaceutics*, **13(4)**, 437 (2021) https://doi.org/10.3390/pharmaceutics13040437.

[9] Naseri M, Golmohamadzadeh S, Arouiee H, Jaafari MR, Nemati SH. Preparation and comparison of various formulations of solid lipid nanoparticles (SLNs) containing essential oil of Zataria multiflora. *Jour of Hor and Posth Res*, **3(1)**,73-84 (2020) https://doi.org/10.22077/jhpr.2019.2570.1068.

[10] Mendoza-Munoz N, Urbán-Morlán Z, Leyva-Gómez G, de la Luz Zambrano-Zaragoza M, Quintanar-Guerrero D. Solid lipid nanoparticles: an approach to improve oral drug delivery. *J Pharm Pharm Sci*, **13(24)**, 509-32 (2021) https://doi.org/10.18433/jpps31788.

[11] Godge G, Randhawan B, Shaikh A, Bharat S, Raskar M, Hiremath S. Formulation Perspectives and Applications of Solid Lipid Nanoparticles for Drug Delivery: A Review. *RGUHS Jour of Pharm Sci*,**14(1)**, (2024) https://doi.org/10.26463/rjps.14_1_7.

[12] Scioli Montoto S, Muraca G, Ruiz ME. Solid lipid nanoparticles for drug delivery: pharmacological and biopharmaceutical aspects. *Front Mol Biosci*, **30(7)**, 319 (2020) https://doi.org/10.3389/fmolb.2020.587997.

[13] Mirchandani Y, Patravale VB, Brijesh S. Solid lipid nanoparticles for hydrophilic drugs. *J Control Release*. **10(335)**, 457-64 (2021) https://doi.org/10.1016/j.jconrel.2021.05.032.

[14] Satapathy MK, Yen TL, Jan JS, Tang RD, Wang JY, Taliyan R, Yang CH. Solid lipid nanoparticles (SLNs): an advanced drug delivery system targeting brain through BBB. *Pharmaceutics*, **13(8)**,1183 (2021) https://doi.org/10.3390/pharmaceutics13081183.

[15] Gupta T, Singh J, Kaur S, Sandhu S, Singh G, Kaur IP. Enhancing bioavailability and stability of curcumin using solid lipid nanoparticles CLEN): A covenant for its effectiveness. *Front Bioeng Biotechnol*, **15(8)**, 879 (2020) https://doi.org/10.3389/fbioe.2020.00879.

[16] Liparulo A, Esposito R, Santonocito D, Muñoz-Ramírez A, Spaziano G, Bruno F, Xiao J, Puglia C, Filosa R, Berrino L, D'Agostino B. Formulation and Characterization of Solid Lipid Nanoparticles Loading RF22-c, a Potent and Selective 5-LO Inhibitor, in a Monocrotaline-Induced Model of Pulmonary Hypertension. *Front pharmacol*, **28(11)**, 83 (2020) https://doi.org/10.3389/fphar.2020.00083.

[17] Musielak E, Feliczak-Guzik A, Nowak I. Optimization of the conditions of solid lipid nanoparticles (SLN) synthesis. *Molecules*, **27(7)**, 2202 (2022) https://doi.org/10.3390/molecules27072202.

[18] E, Cerveri I, Lacedonia D, Paone G, Sanduzzi Zamparelli A, Sorbo R, Allegretti M, Lanata L, Scaglione F. Clinical efficacy of carbocysteine in COPD: beyond the mucolytic action. *Pharmaceutics*, **14(6)**,1261 (2022) https://doi.org/10.3390/pharmaceutics14061261.

[19] Fu Y, Dai A, Dong L, Ning K. Efficacy and Safety of Expectorant/antioxidants in the Treatment of COPD: Network Meta-analysis. *China Pharmacy*, 2778-84 (2021) https://pesquisa.bvsalud.org/portal/resource/pt/wpr-904783.

[20] Ferraro M, Di Vincenzo S, Sangiorgi C, Leto Barone S, Gangemi S, Lanata L, Pace E. Carbocysteine modifies circulating miR-21, IL-8, sRAGE, and fAGEs levels in mild acute exacerbated COPD patients: a pilot study. *Pharmaceuticals*, **15(2)**, 218 (2022) https://doi.org/10.3390/ph15020218.

[21] Zhou L, Liu J, Wang L, He Y, Zhang J. Carbocistein improves airway remodeling in asthmatic mice. *Am J Transl Res*, **14(8)**, 5583 (2022) https://pmc.ncbi.nlm.nih.gov/articles/PMC9452364/.

[22] Rubio MC, de la Serna Blazquez O, Martin JL, Cuetos MR. Carbocysteine as Adjuvant Therapy in Acute Respiratory Tract Infections in Patients without Underlying Chronic Conditions: Systematic Review and Meta-Analysis. *Opn Jou Res Dis*, **14(2)**, 39-50 (2024) https://doi.org/10.4236/ojrd.2024.142004.

[23] Dailah HG. Therapeutic potential of small molecules targeting oxidative stress in the treatment of chronic obstructive pulmonary disease (COPD): a comprehensive review. *Molecules*, **27(17)**, 5542 (2022) https://doi.org/10.3390/molecules27175542.

[24] Kariya S, Okano M, Higaki T, Makihara S, Tachibana T, Nishizaki K. Long-term treatment with clarithromycin and carbocisteine improves lung function in chronic cough patients with chronic rhinosinusitis. *Am J Otolaryngol*, **41(1)**, 102315 (2020) https://doi.org/10.1016/j.amjoto.2019.102315.

[25] Lo Bello F, Ieni A, Hansbro PM, Ruggeri P, Di Stefano A, Nucera F, Coppolino I, Monaco F, Tuccari G, Adcock IM, Caramori G. Role of the mucins in pathogenesis of COPD: implications for therapy. *Expert Rev Respir Med*, **14(5)**, 465-83 (2020) https://doi.org/10.1080/17476348.2020.1739525.

[26] Abdelhamid AM, Youssef ME, Cavalu S, Mostafa-Hedeab G, Youssef A, Elazab ST, Ibrahim S, Allam S, Elgharabawy RM, El-Ahwany E, Amin NA. Carbocisteine as a modulator of Nrf2/HO-1 and NFκB interplay in rats: new inspiration for the revival of an old drug for treating ulcerative colitis. *Front Pharmacol*, **8(13)**, 887233 (2022) https://doi.org/10.3389/fphar.2022.887233.

[27] Bhalekar MR, Madgulkar AR, Desale PS, Marium G. Formulation of piperine solid lipid nanoparticles (SLN) for treatment of rheumatoid arthritis. *Drug Dev Ind Pharm*, **43(6)**, 1003–10 (2017) https://doi.org/10.1080/03639045.2017.1291666.

[28] Rubiano S, Echeverri JD, Salamanca CH. Solid lipid nanoparticles (SLNs) with potential as cosmetic hair formulations made from Otoba wax and ultrahigh pressure homogenization. *Cosmetics*, **7(2)**, 42 (2020) https://doi.org/10.3390/cosmetics7020042.

[29] Steiner D, Bunjes H. Influence of process and formulation parameters on the preparation of solid lipid nanoparticles by dual centrifugation. *Int J Pharm*, **1(3)**, 100085 (2021) https://doi.org/10.1016/j.ijpx.2021.100085.

[30] Kraisit P, Hirun N, Mahadlek J, Limmatvapirat S. Fluconazole-loaded solid lipid nanoparticles (SLNs) as a potential carrier for buccal drug delivery of oral candidiasis treatment using the Box-Behnken design. *J Drug Deliv Sci Technol*, **1(63)**, 102437 (2021) https://doi.org/10.1016/j.jddst.2021.102437.

[31] Khan S, Ullah M, Saeed S, Saleh E, Kassem A, Arbi F, Wahab A, Rehman M, ur Rehman K, Khan D, Zaman U. Nanotherapeutic approaches for transdermal drug delivery systems and their biomedical applications. *Eur Polym J*, **6(2)**, 112819 (2024) https://doi.org/10.1016/j.eurpolymj.2024.112819.

[32] Jai Bharti Sharma, Bhatt S, Tiwari A, Tiwari V, Kumar M, Verma R, et al. Statistical optimization of tetrahydrocurcumin loaded solid lipid nanoparticles using Box Behnken design in the management of streptozotocin-induced diabetes mellitus. *Saudi Pharm J*, **31(9)**, 101727–7 (2023) https://doi.org/10.1016/j.jsps.2023.101727.

[33] Taherzadeh S, Naeimifar A, Yeganeh EM, Esmaili Z, Mahjoub R, Javar HA. Preparation, statistical optimization and characterization of propolis-loaded solid lipid nanoparticles using Box-Behnken design. *Adv Pharm Bull*, **11(2)**, 301 (2021) https://doi.org/10.34172/apb.2021.043.

[34] Devi AR, Vidyavathi M, Suryateja SP. Surface modification of optimized asenapine maleate loaded solid lipid nanoparticles using box-behnken design. *J. Pharm. Res. Int*, **15(33)**, 176-93 (2021) https://doi.org/10.9734/jpri/2021/v33i31B31706.

[35] Singh S, Dobhal AK, Jain A, Pandit JK, Chakraborty S. Formulation and Evaluation of Solid Lipid Nanoparticles of a Water Soluble Drug: Zidovudine. *Chem Pharm Bull*, **58(5)**, 650–5 (2010) https://doi.org/10.1248/cpb.58.650.

[36] Mura P, Maestrelli F, D'Ambrosio M, Luceri C, Cirri M. Evaluation and comparison of solid lipid nanoparticles (SLNs) and nanostructured lipid carriers (NLCs) as vectors to develop hydrochlorothiazide effective and safe pediatric oral liquid formulations. *Pharmaceutics*, **3(4)**, 437 (2021) https://doi.org/10.3390/pharmaceutics13040437.

[37] Khoiriyah M, Perangirangin JM, Kuncahyo I. Fenofibrate Characterization of Solid Lipid Nanoparticles Using the High Shear Homogenization Method. *Nat Sci Eng Tech J*, **2(2)**, 79-86 (2022) https://doi.org/10.37275/nasetjournal.v2i2.21.

[38] Chandana M, Ramana MV, Rao NR. Formulation and evaluation of Valsartan solid lipid nanoparticles. *J Drug Deliv Sci Technol*, **25(11)**, (2-S),103-8 (2021) https://doi.org/10.22270/jddt.v11i2-S.4694.

[39] Nasiri F, Faghfouri L, Hamidi M. Preparation, optimization, and in-vitro characterization of α-tocopherol-loaded solid lipid nanoparticles (SLNs). *Drug Dev Ind Pharm*, **46(1)**, 159-71 (2020) https://doi.org/10.1080/03639045.2019.1711388.

[40] Butani S. Fabrication of an ion-sensitive in situ gel loaded with nanostructured lipid carrier for nose to brain delivery of donepezil. *A Jour Pharm*, **12(04)**, (2018) https://doi.org/10.22377/ajp.v12i04.2838.

[41] Yu S, Wang QM, Wang X, Liu D, Zhang W, Ye T, Yang X, Pan W. Liposome incorporated ion sensitive in situ gels for opthalmic delivery of timolol maleate. *Int J Pharm*, **480(1-2)**,128-36 (2015) https://doi.org/10.1016/j.ijpharm.2015.01.032.

[42] Huang CH, Hu PY, Wu QY, Xia MY, Zhang WL, Lei ZQ, Li DX, Zhang GS, Feng JF. Preparation, in vitro and in vivo Evaluation of Thermosensitive in situ Gel Loaded with Ibuprofen-Solid Lipid Nanoparticles for Rectal Delivery. *Drug Des Devel Ther*, **31**, 1407-31 (2023) https://doi.org/10.2147/DDDT.S350886.

[43] Tatke A, Dudhipala N, Janga KY, Balguri SP, Avula B, Jablonski MM, Majumdar S. In situ gel of triamcinolone acetonide-loaded solid lipid nanoparticles for improved topical ocular delivery: tear kinetics and ocular disposition studies. *Nanomaterials*, **9(1)**, 33, (2018) https://doi.org/10.3390/nano9010033.

[44] Janga KY, Tatke A, Balguri SP, Lamichanne SP, Ibrahim MM, Maria DN, Jablonski MM, Majumdar S. Ion-sensitive in situ hydrogels of natamycin bilosomes for enhanced and prolonged ocular pharmacotherapy: in vitro permeability, cytotoxicity and in vivo evaluation. *Artif Cells Nanomed Biotechnol*, **31, 46** (sup1), 1039-50 (2018) https://doi.org/10.1080/21691401.2018.1443117.

[45] Lynch CR. Development and characterization of a solid lipid nanoparticle-loaded thermosensitive gel for the delivery of timolol to the eye (Doctoral dissertation, Department of Ophthalmology, Faculty of Health Sciences, University of the Witwatersrand, South Africa) https://hdl.handle.net/10539/34840.

[46] Okur NÜ, Yağcılar AP, Siafaka PI. Promising polymeric drug carriers for local delivery: the case of in situ gels. *Curr Drug Deliv*, **17(8)**, 675-93 (2020) https://doi.org/10.2174/1567201817666200608145748.

[47] Uppuluri CT, Ravi PR, Dalvi AV. Design, optimization and pharmacokinetic evaluation of Piribedil loaded solid lipid nanoparticles dispersed in nasal in situ gelling system for effective management of Parkinson's disease. *Int J Pharm*, **606**, 120881 (2021) https://doi.org/10.1016/j.ijpharm.2021.120881.

[48] Sun K, Hu K. Preparation and characterization of tacrolimus-loaded SLNs in situ gel for ocular drug delivery for the treatment of immune conjunctivitis. *Drug Des Devel Ther*, **12**, 141 (2021) https://doi.org/10.2147/DDDT.S287721.

[49] Sun Y, Li L, Xie H, Wang Y, Gao S, Zhang L, Bo F, Yang S, Feng A. Primary studies on construction and evaluation of ion-sensitive in situ gel loaded with paeonol-solid lipid nanoparticles for intranasal drug delivery. *Int J Nanomedicine*, **4**, 3137-60 (2020) https://doi.org/10.2147/IJN.S247935.

[50] Amkar AJ, Rane BR, Jain AS. Development and Evaluation of Nanosuspension Loaded Nanogel of Nortriptyline HCl for Brain Delivery. *Eng Proc*, **56(1)**, 58 (2023) https://doi.org/10.3390/ASEC2023-15311.

[51] Elkarray SM, Farid RM, Abd-Alhaseeb MM, Omran GA, Habib DA. Intranasal repaglinide-solid lipid nanoparticles integrated in situ gel outperform conventional oral route in hypoglycemic activity. *J Drug Deliv Sci Technol*, **68**, 103086 (2022) https://doi.org/10.1016/j.jddst.2021.103086.

[52] Das T, Venkatesh MP, Kumar TP, Koland M. SLN based alendronate in situ gel as an implantable drug delivery system–A full factorial design approach. *J Drug Deliv Sci Technol*, **55**, 101415 (2020) https://doi.org/10.1016/j.jddst.2019.101415.

[53] Ahmed TA, Badr-Eldin SM, Ahmed OA, Aldawsari H. Intranasal optimized solid lipid nanoparticles loaded in situ gel for enhancing trans-mucosal delivery of simvastatin. *J Drug Deliv Sci Technol*, **1(48)**, 499-508 (2018) https://doi.org/10.1016/j.jddst.2018.10.027.

[54] Mohanty D, Alsaidan OA, Zafar A, Dodle T, Gupta JK, Yasir M, Mohanty A, Khalid M. Development of atomoxetine-loaded NLC in situ gel for nose-to-brain delivery: optimization, in vitro, and preclinical evaluation. *Pharmaceutics*, **15(7)**, 1985 (2023) https://doi.org/10.3390/pharmaceutics15071985.

[55] Abbas H, Refai H, El Sayed N. Superparamagnetic iron oxide–loaded lipid nanocarriers incorporated in thermosensitive in situ gel for magnetic brain targeting of clonazepam. *J Pharm Sci* , **107(8)**, 2119-27 (2018) https://doi.org/10.1016/j.xphs.2018.04.007.

[56] Gade S, Patel KK, Gupta C, Anjum MM, Deepika D, Agrawal AK, Singh S. An ex vivo evaluation of moxifloxacin nanostructured lipid carrier enriched in situ gel for transcorneal permeation on goat cornea. *J Pharm Sci*, **108(9)**, 2905-16 (2019) https://doi.org/10.1016/j.xphs.2019.04.005.

[57] Bondre RM, Kanojiya PS, Wadetwar RN, Kangali PS. Sustained vaginal delivery of in situ gel containing Voriconazole nanostructured lipid carrier: formulation, in vitro and ex vivo evaluation. *J Dispers Sci Technol*, **44(8)**, 1466-78 (2023) https://doi.org/10.1080/01932691.2021.2022489.

[58] Tripathi D, Sonar PK, Parashar P, Chaudhary SK, Upadhyay S, Saraf SK. Augmented brain delivery of cinnarizine through nanostructured lipid carriers loaded in situ gel: in vitro and pharmacokinetic evaluation. *BioNanoScience*, **11(1)**, 159-71 (2021) https://doi.org/10.1007/s12668-020-00821-2.

[59] Li JC, Zhang WJ, Zhu JX, Zhu N, Zhang HM, Wang X, Zhang J, Wang QQ. Preparation and brain delivery of nasal solid lipid nanoparticles of quetiapine fumarate in situ gel in rat model of schizophrenia. *Int J clin exp med*, **8(10)**, 17590 (2015) https://pubmed.ncbi.nlm.nih.gov/26770349/.

[60] Chen P, Zhang H, Cheng S, Zhai G, Shen C. Development of curcumin loaded nanostructured lipid carrier based

thermosensitive in situ gel for dermal delivery. *Colloids Surf A Physicochem Eng Asp*, **5, 506**, 356-62 (2016) https://doi.org/10.1016/j.colsurfa.2016.06.054.

[61] Aboud HM, El Komy MH, Ali AA, El Menshawe SF, Abd Elbary A. Development, optimization, and evaluation of carvedilol-loaded solid lipid nanoparticles for intranasal drug delivery. *AAPS pharmscitech*, **17**, 1353-65 (2016) https://doi.org/10.1208/s12249-015-0440-8.

[62] Rajput AP, Butani SB. Resveratrol anchored nanostructured lipid carrier loaded in situ gel via nasal route: Formulation, optimization and in vivo characterization. *J Drug Deliv Sci Technol*, **51**, 214-23 (2019) https://doi.org/10.1016/j.jddst.2019.01.040.

[63] Abdelbary A, Salem HF, Khallaf RA, Ali AM. Mucoadhesive niosomal in situ gel for ocular tissue targeting: in vitro and in vivo evaluation of lomefloxacin hydrochloride. *Pharm Dev Technol*, **22(3)**, 409-17 (2017) https://doi.org/10.1080/10837450.2016.1219916.

[64] Wavikar PR, Vavia PR. Rivastigmine-loaded in situ gelling nanostructured lipid carriers for nose to brain delivery. *J Liposome Res*, **25(2)**, 141-9 (2015) https://doi.org/10.3109/08982104.2014.954129.

[65] Mahmoud RA, Hussein AK, Nasef GA, Mansour HF. Oxiconazole nitrate solid lipid nanoparticles: formulation, in-vitro characterization and clinical assessment of an analogous loaded carbopol gel. *Drug Dev Ind Pharm*, **46(5)**, 706-16 (2020) https://doi.org/10.1080/03639045.2020.1752707.